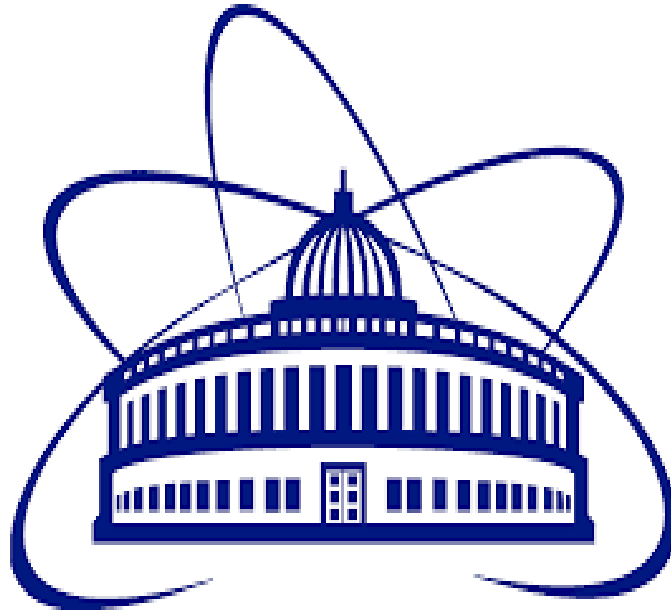


Role of Active Gluons in Hadron Interactions at High Multiplicity

Participant: Shahzaib Abbas



JOINT INSTITUTE FOR NUCLEAR RESEARCH

Veksler and Baldin Laboratory of High Energy Physics

Supervisor: Dr. Elena Kokoulina

Participation period: 03 March - 20 April 2025

Wave: 12

Abstract

The investigation of multiparticle processes is essential for deepening our understanding of fundamental particles and contributes to the pursuit of a grand unified theory that aims to merge the four fundamental forces of nature. This report focuses on two key processes: electron-positron annihilation and proton-antiproton pair annihilation, with particular emphasis on the latter. These processes involve complex mathematical structures and advanced concepts in particle physics, including group theory and gauge theories with local symmetries. Gluons, which mediate the strong force, are central to this study. To examine the produced particles, their multiplicity distributions have been analyzed through both experimental and theoretical approaches within the framework of quantum chromodynamics. Several theoretical models have been proposed, among which the two-stage model is the most widely recognized. Furthermore, particle detection methods employed at JINR are discussed in detail. The experimental data analysis was performed using the CERN Root software.

Acknowledgements

I am deeply grateful to JINR, Russia, for granting me this incredible opportunity to work at such a prestigious institute. It is a true honor to have Dr. Elena Kokouline as my mentor—her steadfast guidance and support were instrumental in bringing this project to completion. Undertaking this project has been a transformative journey, allowing me to delve deeply into particle physics and cultivate a profound passion for the field. From learning the intricacies of QCD-inspired models to applying advanced computational tools like CERN ROOT, every challenge has sharpened my analytical skills and deepened my appreciation for theoretical and experimental synergy. This experience has not only expanded my knowledge but also inspired me to contribute meaningfully to the future of high-energy physics research.

Contents

1	Fundamentals of Multiplicity Distributions I	5
1.1	Introduction	5
1.2	QCD jets in the framework of Markov branching processes	6
1.2.1	Basic Mechanisms Governing QCD Jets	6
1.3	Jet Evolution via Generating Functions	6
2	Fundamentals of Multiplicity Distributions II	9
2.1	Equations Describing the Evolution of QCD Jets	9
2.2	Explicit results in certain situations	10
2.2.1	Gluon Jet	11
2.2.2	Quark Jet	12
3	Electron-Positron Annihilation	13
3.1	Distribution function	13
3.2	Fitting e^+e^- Data	14
4	Proton-Proton Interaction	17
4.1	Proton-Proton Collision Framework	17
4.2	Fission of Gluons in the I-Scheme	18
4.2.1	Manifestation of Free Gluons	18
4.2.2	Creation of Fission Gluons	19
4.2.3	Hadronization	19
4.3	Fitting pp	19
4.3.1	Involving Gluon Fission	21
4.4	Proton-Antiproton Annihilation	23
5	Conclusion	24
6	Bibliography	25
7	Appendix	26

Chapter 1

Fundamentals of Multiplicity Distributions I

1.1 Introduction

In recent years, particle physics has gained remarkable popularity, with an increasing number of accelerators and high-energy projects being developed. As energy levels rise, new decay channels are uncovered, leading to the discovery of previously unknown particles. This progress has driven the creation of new theories and models, including quantum chromodynamics (QCD). Exploring the strong interaction offers valuable insights into the fundamental nature of matter and energy.

A major challenge in high energy physics is the production of a large number of secondary particles. Multiparticle production holds valuable information about the nature of the strong interaction, and its analysis relies heavily on statistical methods. Through the study of these processes, the phenomenon of jets was discovered. Jets can be investigated in any interaction involving energetic partons (quarks and gluons), though they are most commonly studied in high-energy e^+e^- annihilation.

$$e^+e^- \rightarrow \gamma/Z^0 \rightarrow \bar{q}q$$

The initial stage of parton evolution at high energies, known as *the cascade stage*, is described by perturbative QCD. As parton energies decrease, they hadronize into observable particles in *the hadronization stage*, which lies beyond perturbative QCD. Konishi, Ukawa, and Veneziano studied multiparton spectra in QCD jets, showing that gluon jets are softer than quark jets and exhibit an ordering among final-state partons.

1.2 QCD jets in the framework of Markov branching processes

1.2.1 Basic Mechanisms Governing QCD Jets

In the study of multiparticle production at high energies, QCD jets are treated as Markov branching processes, with the QCD evolution parameter interpreted as the natural evolution variable governing the process.

$$Y = \frac{1}{2\pi b} \ln \left[1 + \alpha b \ln \left(\frac{Q^2}{\mu^2} \right) \right] \quad (1)$$

where $2\pi b = \frac{1}{6}(11N_c - 2N_f)$ for a theory with N_c colors and N_f flavors, as the thickness value of a quark or a gluon that gives rise to a gluon or a quark jet.

There are three main elementary processes that contribute to the overall gluon or quark distribution inside QCD jets with different weights:

- *gluon fission*: $g \rightarrow g + g$, with $A\Delta Y$ denoting the probability that a gluon in the infinitesimal interval ΔY will transform into two gluons
- *quark bremsstrahlung*: $q \rightarrow q + g$, with $\tilde{A}\Delta Y$ denoting the probability that a quark in the infinitesimal interval ΔY will radiate a gluon with the quark continuing on its original trajectory with modified energy and momentum
- *quark pair creation*: $g \rightarrow q + \bar{q}$, with $B\Delta Y$ denoting the probability that a quark-antiquark pair in the infinitesimal interval ΔY will be created from a gluon

We assume that A , \tilde{A} , and B are Y -independent constants and that each individual parton acts independently from the others, always with the same infinitesimal probability.

1.3 Jet Evolution via Generating Functions

We introduce the infinitesimal generating functions for gluon jet and quark jet, respectively, as

$$w^{(g)}(u_g, u_q) = \sum_{m_g, m_q=0}^{\infty} a_{m_g, m_q}^{(g)} u_g^{m_g} u_q^{m_q} = (-A - B)u_g + Au_g^2 + Bu_q^2 \quad (2)$$

$$w^{(q)}(u_g, u_q) = \sum_{m_g, m_q=0}^{\infty} a_{m_g, m_q}^{(q)} u_g^{m_g} u_q^{m_q} = -\tilde{A}u_q + \tilde{A}u_q u_g \quad (3)$$

Let us denote by $P_{m_g, m_q; n_g, n_q}(Y)$ the probability that a system initially containing m_g gluons and m_q quarks evolves into a final state with n_g gluons and n_q quarks over a jet of thickness Y . Accordingly, the probability generating function for a *gluon jet* is defined as:

$$G(u_g, u_q; Y) = \sum_{n_g, n_q=0}^{\infty} P_{1,0; n_g, n_q}(Y) u_g^{n_g} u_q^{n_q} \quad (4)$$

and the probability generating function for a *quark jet* is given by

$$Q(u_g, u_q; Y) = \sum_{n_g, n_q=0}^{\infty} P_{0,1; n_g, n_q}(Y) u_g^{n_g} u_q^{n_q} \quad (5)$$

When examining the evolution of the total parton population, which consists of both gluons and quarks, through a thickness Y , a probabilistic approach enables us to treat this population as composed of independent sub-populations. Each sub-population behaves as though it originates from a single initial quark or gluon. Therefore, the overall evolution can be understood as the sum of independent parton populations, each initialized with one quark or gluon. This can be mathematically expressed as follows:

$$\sum_{n_g, n_q}^{\infty} P_{m_g, m_q; n_g, n_q}(Y) u_g^{n_g} u_q^{n_q} = [G(u_g, u_q; Y)]^{m_g} [Q(u_g, u_q; Y)]^{m_q} \quad (6)$$

Since the process is homogeneous in Y , the transition probabilities obey Chapman-Kolmogorov equations:

$$P_{m_g, m_q; n_g, n_q}(Y + Y') = \sum_{l_g, l_q}^{\infty} P_{m_g, m_q; l_g, l_q}(Y) P_{l_g, l_q; n_g, n_q}(Y') \quad (7)$$

For a gluon jet, we get

$$P_{0,1; n_g, n_q}(Y + Y') = \sum_{l_g, l_q}^{\infty} P_{1,0; l_g, l_q}(Y) P_{l_g, l_q; n_g, n_q}(Y') \quad (8)$$

and for a quark jet, we get

$$P_{1,0;n_g,n_q}(Y + Y') = \sum_{l_g,l_q}^{\infty} P_{0,1;l_g,l_q}(Y) P_{l_g,l_q;n_g,n_q}(Y') \quad (9)$$

From (6) and (7), we get

$$G(u_g, u_q; Y + Y') = G[G(u_g, u_q; Y'), Q(u_g, u_q; Y'); Y] \quad (10)$$

$$Q(u_g, u_q; Y + Y') = Q[G(u_g, u_q; Y'), Q(u_g, u_q; Y'); Y] \quad (11)$$

From (2)–(5), we can see that

$$G(u_g, u_q; \Delta Y) = u_g + w^{(g)}(u_g, u_q) \Delta Y + \mathcal{O}(\Delta Y) \quad (12)$$

$$Q(u_g, u_q; \Delta Y) = u_q + w^{(q)}(u_g, u_q) \Delta Y + \mathcal{O}(\Delta Y) \quad (13)$$

Substituting (12) and (13) into (10) and (11), while substituting Y' with ΔY , then dividing both sides by ΔY and letting $\Delta Y \rightarrow 0$, we obtain

$$\frac{\partial G(u_g, u_q; Y)}{\partial Y} = \frac{\partial G}{\partial u_g} w^{(g)}(u_g, u_q) + \frac{\partial G}{\partial u_q} w^{(q)}(u_g, u_q) \quad (14)$$

$$\frac{\partial Q(u_g, u_q; Y)}{\partial Y} = \frac{\partial Q}{\partial u_g} w^{(g)}(u_g, u_q) + \frac{\partial Q}{\partial u_q} w^{(q)}(u_g, u_q) \quad (15)$$

Chapter 2

Fundamentals of Multiplicity Distributions II

2.1 Equations Describing the Evolution of QCD Jets

We can recognize the forward Kolmogorov equations for the generating functions of the transition probability $P_{m_g, m_q; n_g, n_q}(Y)$ in (17) and (18). The corresponding backward Kolmogorov equations follow from (13) and (14):

$$\frac{\partial G}{\partial Y} = w^{(g)} [G(u_g, u_q; Y), Q(u_g, u_q; Y)] \quad (16)$$

$$\frac{\partial Q}{\partial Y} = w^{(q)} [G(u_g, u_q; Y), Q(u_g, u_q; Y)] \quad (17)$$

Substituting (2) and (3) into (16) and (17), we obtain

$$\frac{\partial G}{\partial Y} = -AG + AG^2 - BG + BQ^2 \quad (18)$$

$$\frac{\partial Q}{\partial Y} = -\tilde{A}Q + \tilde{A}QG \quad (19)$$

We can find the probability for a gluon or a quark to produce n_g gluons and n_q quarks in the interval $Y + \Delta Y$ through the main elementary processes. For a gluon jet

$$\begin{aligned}
P_{1,0;n_g,n_q}(Y + \Delta Y) &= (1 - \tilde{A}n_q\Delta Y - An_g\Delta Y - Bn_g\Delta Y)P_{1,0;n_g,n_q}(Y) \\
&\quad + \tilde{A}n_q\Delta Y P_{1,0;n_g-1,n_q}(Y) + A(n_g - 1)\Delta Y P_{1,0;n_g-1,n_q}(Y) \\
&\quad + B(n_g + 1)\Delta Y P_{1,0;n_g+1,n_q-2}(Y) + \mathcal{O}(\Delta Y)
\end{aligned} \tag{20}$$

Dividing both sides by ΔY and letting $\Delta Y \rightarrow 0$, we obtain the following system of differential equations

$$\begin{aligned}
\frac{dP_{1,0;n_g,n_q}(Y)}{dY} &= (-\tilde{A}n_q - An_g - Bn_g)P_{1,0;n_g,n_q}(Y) \\
&\quad + \tilde{A}n_q P_{1,0;n_g-1,n_q}(Y) + A(n_g - 1)P_{1,0;n_g-1,n_q}(Y) \\
&\quad + B(n_g + 1)P_{1,0;n_g+1,n_q-2}(Y)
\end{aligned} \tag{21}$$

For the gluon exclusive cross-sections in a gluon jet or a quark jet, we respectively have the following

$$\frac{dP_{1,0;n_g,0}(Y)}{dY} = (-A - B)n_g P_{1,0;n_g,0}(Y) + A(n_g - 1)P_{1,0;n_g-1,0}(Y) \tag{22}$$

$$\begin{aligned}
\frac{dP_{0,1;n_g,1}(Y)}{dY} &= -\tilde{A}P_{0,1;n_g,1}(Y) - (B + A)n_g P_{0,1;n_g,1}(Y) \\
&\quad + \tilde{A}P_{0,1;n_g-1,1}(Y) + A(n_g - 1)P_{0,1;n_g-1,1}(Y)
\end{aligned} \tag{23}$$

The corresponding generating functions are

$$\frac{\partial G}{\partial Y} = -AG + AG^2 - BG \tag{24}$$

$$\frac{\partial Q}{\partial Y} = -\tilde{A}Q + \tilde{A}QG \tag{25}$$

2.2 Explicit results in certain situations

While obtaining explicit solutions in terms of the generating functions (24) and (25), or of the exclusive cross sections, (20), is generally challenging, it is possible to derive approximate solutions for specific cases. These approximations prove to be particularly intriguing and contribute to a deeper comprehension of the overall problem.

We make the approximation $B = 0$, $A \neq \tilde{A} \neq 0$, meaning that we don't allow gluons to split into quark-antiquark pairs. In other words, from the definition of B , there is no room for flavors in the theory. Then (24) and (25) become

$$\frac{\partial G}{\partial Y} = -AG + AG^2 \quad (26)$$

$$\frac{\partial Q}{\partial Y} = -\tilde{A}Q + \tilde{A}QG \quad (27)$$

The gluon exclusive cross-sections in a gluon jet or a quark jet satisfy the following

$$\frac{dP_{1,0;n_g,0}(Y)}{dY} = -An_g P_{1,0;n_g,0}(Y) + A(n_g - 1)P_{1,0;n_g-1,0}(Y) \quad (28)$$

$$\begin{aligned} \frac{dP_{0,1;n_g,1}(Y)}{dY} &= -\tilde{A}P_{0,1;n_g,1}(Y) - An_g P_{0,1;n_g,1}(Y) \\ &+ \tilde{A}P_{0,1;n_g-1,1}(Y) + A(n_g - 1)P_{0,1;n_g-1,1}(Y) \end{aligned} \quad (29)$$

with the following initial conditions

$$P_{1,0;1,0}(0) = 1, \quad P_{1,0;n_g,0}(0) = 0, \quad \forall n_g > 1 \quad (30)$$

$$P_{0,1;0,1}(0) = 1, \quad P_{0,1;n_g,1}(0) = 0, \quad \forall n_g \geq 1 \quad (31)$$

2.2.1 Gluon Jet

From (28) and (30), we obtain

$$P_{1,0;1,0}(Y) = e^{-AY} \quad (32)$$

$$P_{1,0;n_g,0}(Y) = e^{-AY} (1 - e^{-AY})^{n_g-1}, \quad (33)$$

where the average gluon multiplicity is $\langle n_g \rangle = e^{AY}$.

The normalized exclusive cross-section for producing n_g gluons is

$$\frac{\sigma_{n_g}^{(g,0)}}{\sigma_{tot}} = P_{1,0;n_g,0}(Y) = \frac{1}{\langle n_g \rangle} \left(1 - \frac{1}{\langle n_g \rangle} \right)^{n_g-1} \quad (34)$$

which corresponds to a Furry-Yule distribution. The variance is

$$D^2 = e^{AY} (e^{AY} - 1) \quad (35)$$

Thus we can obtain the second correlative moment to be

$$f_2 = e^{2AY} - 2e^{AY} \quad (36)$$

and the corresponding generating function is

$$G = \sum_{n_g=0}^{\infty} u_g^{n_g} P_{1,0;n_g,0}(Y) = \frac{u_g e^{-AY}}{1 - u_g(1 - e^{-AY})} \quad (37)$$

2.2.2 Quark Jet

From (29) and (31), we obtain

$$P_{0,1;0,1}(Y) = e^{-\tilde{A}Y} \quad (38)$$

$$P_{0,1;n_g,1}(Y) = \frac{\mu(\mu+1)\cdots(\mu+n_g-1)}{n_g!} e^{-\tilde{A}Y} (1 - e^{-AY})^{n_g}, \quad (39)$$

where $\mu = \frac{\tilde{A}}{A}$ and the average gluon multiplicity is $\langle n_g \rangle = \mu(e^{AY} - 1)$. We have the variance as

$$D^2 = \mu e^{AY} (e^{AY} - 1) \quad (40)$$

We obtain the second correlative moment to be

$$f_2 = \frac{\langle n_g \rangle^2}{\mu} \quad (41)$$

Then the normalized exclusive cross-section for producing n_g gluons is

$$\frac{\sigma_{n_g}^{(0,q)}}{\sigma_{tot}} = P_{0,1;n_g,1}(Y) = \frac{\mu(\mu+1)\cdots(\mu+n_g-1)}{n_g!} \left[\frac{\langle n_g \rangle}{\langle n_g \rangle + \mu} \right]^{n_g} \left[\frac{\mu}{\langle n_g \rangle + \mu} \right]^{\mu} \quad (42)$$

This is a Polya-Egenberger distribution, where μ takes half-integer values.

The corresponding generating function is

$$Q = \sum_{n_g=0}^{\infty} u_g^{n_g} u_q P_{0,1;n_g,1}(Y) = u_q \left[\frac{e^{-AY}}{1 - u_g(1 - e^{-AY})} \right]^{\mu} \quad (43)$$

Chapter 3

Electron-Positron Annihilation

3.1 Distribution function

Previously, we investigated the process of e^+e^- annihilation leading to the formation of quark and gluon jets.

$$e^+e^- \rightarrow \gamma(Z^0) \rightarrow q\bar{q} \rightarrow qg\text{-cascade}$$

Within our framework, the quark-gluon cascade was described using Markov branching processes as the fundamental method. Initially, we accounted for three principal elementary processes in QCD: gluon fission, quark gluon emission by a quark and quark-antiquark pair creation [5]. According to our model, the gluon jet in the stage of partons cascade fission is described by negative binomial distribution

$$P_m = \frac{\mu(\mu+1)\cdots(\mu+m-1)}{m!} \left(\frac{\mu}{\mu+\bar{m}}\right)^\mu \left(\frac{\bar{m}}{\mu+\bar{m}}\right)^m \quad (44)$$

In this context, μ represents the ratio of the probabilities of quark bremsstrahlung to gluon fission, \bar{m} denotes the average number of produced gluons, and P_m corresponds to the probability of producing m gluons.

The second stage, hadronization, is modeled by a sub-narrow binomial distribution. This selection is based on the analysis of experimental data from e^+e^- annihilation at energies below 9 GeV, where a negative second correlation moment is observed. The hadronic multiparticle distribution is expressed as:

$$P_n^H = C_N^n \left(\frac{\bar{n}^h}{N}\right)^n \left(1 - \frac{\bar{n}^h}{N}\right)^{N-n} \quad (45)$$

where C_N^n is the binomial coefficient, \bar{n}^h the average hadron yield per parton, and N the maximum number of secondaries.

The convolution of these two stages — the cascade and hadronization — determines the multiparticle distribution of hadrons in e^+e^- annihilation. The probability of obtaining a certain number n of produced charged particles from m partons at the hadronization stage is given by

$$P_n = \Omega \sum_{m=0}^{M_G} \frac{\mu(\mu+1)\cdots(\mu+m-1)}{m!} \left(\frac{\mu}{\mu+\bar{m}}\right)^\mu \left(\frac{\bar{m}}{\mu+\bar{m}}\right)^m \times C_{(2+\alpha m)N}^n \left(\frac{\bar{n}^h}{N}\right)^n \left(1 - \frac{\bar{n}^h}{N}\right)^{(2+\alpha m)N-n} \quad (46)$$

where $C_{(2+\alpha m)N}^n$ is binomial coefficient that equals to

$$C_{(2+\alpha m)N}^n = \frac{(2+\alpha m)N((2+\alpha m)N-1)\cdots((2+\alpha m)N-n+1)}{n!} \quad (47)$$

and parameter α was included to distinguish hadrons produced from quark or gluon.

3.2 Fitting e^+e^- Data

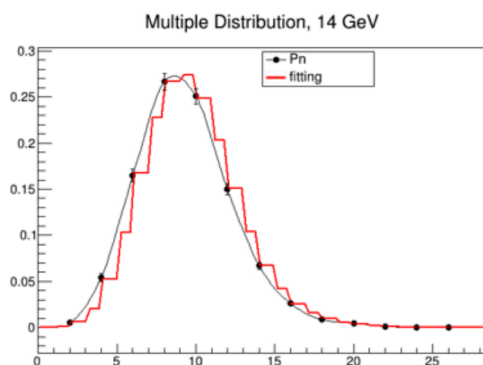
The multiplicity distribution given in equation (3) involves six parameters:

- μ represents the ratio of probabilities between quark bremsstrahlung ($q \rightarrow q + g$) and gluon fission ($g \rightarrow g + g$)
- \bar{m} denotes the average gluon multiplicity
- \bar{n}_h indicates the average number of hadrons generated by a single gluon
- N specifies the maximum possible number of hadrons that can be produced from one gluon
- α defines the ratio of the average number of gluons to quarks produced (\bar{n}_g/\bar{n}_q)
- Ω serves as the normalization coefficient

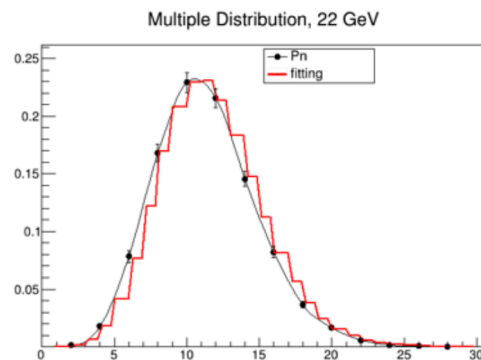
It is evident that the final parameter, Ω , must be equal to 2 due to charge conservation. While the model and calculations allow for any number of produced particles (both even and odd), in reality, the production of an odd number of charged particles is forbidden. Since the initial system is electrically neutral before the collision, it must remain neutral after hadronization as well. This implies that all charged particles should be produced in pairs (one positive and one negative), and thus, probabilities corresponding to odd values of n are excluded from consideration.

We performed the fit for function (3) and determined the parameters using the Fumili2 minimization package from CERN ROOT. The data were obtained from [1]. The fitting procedure was carried out for four different energies: 14, 22, 34.8, and 43.6 GeV. The C++ script used for the fitting is provided in the Appendix.

The results of the fitting are presented in Figures 1-4, where the red line represents the fitted equation and the black line displays the corresponding experimental data along with their uncertainties. The derived parameters for each energy are summarized in Table 3.1.

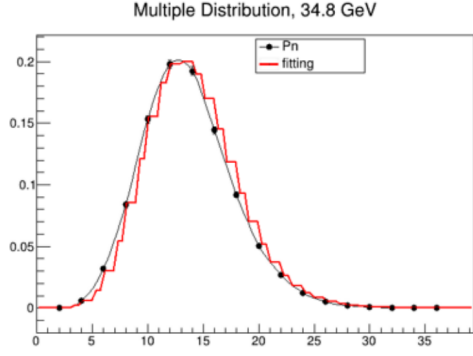


(a) Fig: 1

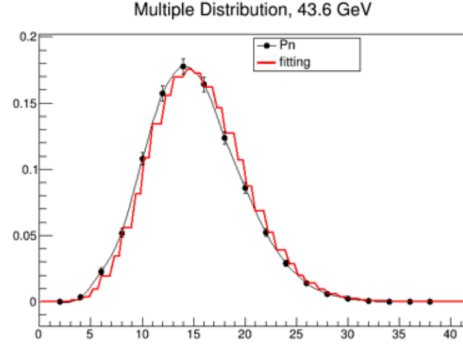


(b) Fig: 2

Figures 1-2: Distribution function for e^+e^- annihilation. The fitted function is shown in red line, the experimental data [1] are shown with black points (the curves are to guide the eye). Left: distribution for 14 GeV. Right: distribution for 22 GeV.



(a) Fig: 3



(b) Fig: 4

Figures 3-4: Distribution function for e^+e^- annihilation. The fitted function is shown in red line, the experimental data [1] are shown with black points (the curves are to guide the eye). Left: distribution for 34.8 GeV. Right: distribution for 43.6 GeV

Table 3.1: Results of fitting - obtained parameters for different energies.

Energy \sqrt{s} , GeV	14	22	34.8	43.6
μ	279219	3.174	0.6836	51.83
\bar{m}	0.0813	1.954	3.214	9.724
\bar{n}^h	4.468	4.675	6.038	2.427
N	27.85	27.8	402856	5.565
α	0.9792	0.21395	0.08254	0.4353
Ω	1.99666	1.99914	2.01421	2.00133
NDF	7	8	12	13
χ^2	2.75432	1.66254	6.22071	5.38212

Chapter 4

Proton-Proton Interaction

4.1 Proton-Proton Collision Framework

The proton-proton interaction leads to the production of particles with high multiplicity, where $n \gg \bar{n}$, and is a collective phenomenon in the high multiplicity regime. Particles such as π^+ , π^0 , and π^- are generated.

When discussing pp interactions, two key features must be considered:

- Each quark may exhibit a branching narrow binomial distribution.
- Each gluon may follow a Furry distribution.

$$Q = \left[1 + \frac{\bar{m}}{\mu} (1 - z)^{-\mu} \right]^6 [G(z)]^{n_g} \quad (48)$$

Gluons are the only participants in multiparticle processes, while quarks remain as spectators.

Next, we will examine two important examples of pp reactions:

$$p + p \rightarrow \pi^+ + n + p$$

$$p + p \rightarrow \pi^0 + p \rightarrow \pi^+ + n + p$$

For quarks and gluons, the multiplicity distribution can be written as:

$$P_m = \frac{\bar{m} e^{-\bar{m}}}{m!} \quad (49)$$

The equation for the simple scheme is:

$$Q(z) = \sum_{m=0}^{\infty} \frac{\bar{m}^m e^{-\bar{m}}}{m!} \left[1 + \frac{\bar{n}^h}{N} (z - 1) \right]^{mN} \quad (50)$$

where \bar{n}^h is the average multiplicity of hadrons which form single gluon and N is the maximum number of hadrons that can be created from a single gluon.

The content of weak gluons is just 50 percent of the total number formed. They are glued to valence quarks of secondary particles and give them mass. We see that:

$$q + g \rightarrow q + \gamma \quad (\text{Compton Scattering})$$

4.2 Fission of Gluons in the I-Scheme

We shall now discuss the I-scheme of gluon fission which has three stages to it. They are:

4.2.1 Manifestation of Free Gluons

Its multiplicity distribution function is denoted by the expression:

$$P_m = \sum_{k=1}^{\infty} e^{-\bar{k}} \frac{\bar{k}^k}{k!} \sum_{n=2}^{\infty} \frac{1}{\bar{m}^k} \frac{(m-1)(m-2)\cdots(m-k)}{(k-1)!} \left(1 - \frac{1}{\bar{m}}\right)^{m-k} C_{\alpha m N}^{\bar{m}-k} \left(\frac{\bar{n}^h}{N}\right)^{n-2} \left(1 - \frac{\bar{n}^h}{N}\right)^{\alpha m N - (n-2)} \quad (51)$$

Now,

$$\sum_{k=0}^{\infty} e^{-\bar{k}} \frac{\bar{k}^k}{k!} = 1 \quad (52)$$

corresponds to the Poisson Distribution.

$$\sum \frac{1}{\bar{m}^k} \frac{(m-1)(m-2)\cdots(m-k)}{(k-1)!} \left(1 - \frac{1}{\bar{m}}\right)^{m-k}$$

corresponds to the Furry Distribution of the gluon jet. Lastly,

$$C_{\alpha m N}^{\bar{m}-k} \left(\frac{\bar{n}^h}{N}\right)^{n-2} \left(1 - \frac{\bar{n}^h}{N}\right)^{\alpha m N - (n-2)}$$

This corresponds to the Binomial Distribution at the hadronization stage.

If $k = 0$, the expression explicitly shows that the primary sources of secondary particles are active gluons rather than valence quarks, where \bar{k} represents the average number of gluons at the moment of collision, and m is the average number of gluons after fission. Among all events, we focus on those with the maximum number of hadrons, denoted by N . Although the number of gluon fissions is large, the number of hadrons produced is constrained, as not all gluons result in hadrons — some remain in quark-gluon systems.

Sources of soft photons predominantly produce secondary particles. The two protons act as leading particles, remaining conserved and not disappearing. In the expression $C_{\alpha m N}^{n-2}$, the term αm represents the actual number of gluons that convert into hadrons.

4.2.2 Creation of Fission Gluons

The Furry distribution is employed to determine the number of gluons that do not participate in gluon fission. Our primary interest lies in the gluons produced after fission. Based on experimental data, the following average values are obtained: $\bar{u} = 2.5$, $\bar{m} = 2.6$, $\bar{n} = 2.5$, $N = 40$, and $\sqrt{s} = 10$ GeV.

An analysis of the data reveals that high-multiplicity events are extremely rare, occurring with very low probabilities.

The presence of multiple gluons enables the production of numerous quark–antiquark pairs, which subsequently form hadrons. Within this quark–gluon system, the formation of baryons and mesons occurs with equal probability, and the ratio of their production increases as the energy approaches unity.

4.2.3 Hadronization

The last and final stage is the hadronization process. It can be measured and analysed accurately with the help of different hadronization parameters.

4.3 Fitting pp

The obtained function has 4 parameters:

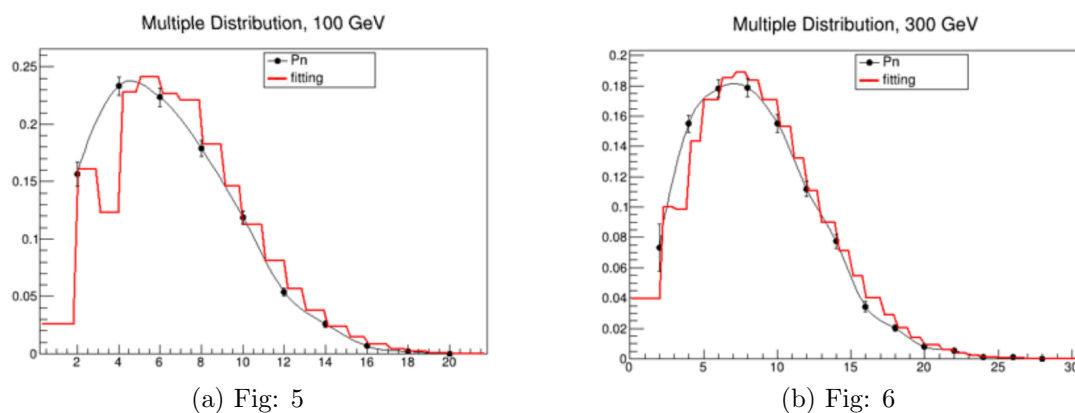
- Ω is a coefficient of normalization (must equal 2 as for e^+e^- annihilation)
- \bar{m} is an average multiplicity of gluons
- \bar{n}^h is an average multiplicity of hadrons produced

- N is the maximum possible number of hadrons produced from 1 gluon

The fitting was performed using the same tools as described previously. Data at 100 GeV were taken from [?], while results at 300 GeV were based on [?]. To obtain probabilities instead of cross sections, one can use:

$$P_n = \frac{\sigma_n}{\sum_n \sigma_n} = \frac{\sigma_n}{\sigma_{\text{total}}} \quad (53)$$

Results of fitting are shown in Figures 6-7. The red line represents the fitting equation and the black one corresponds to experimental data with errors. Modeled parameters for each energy are given in Table 4.1.



Figures 5-6: Function of multiparticle distribution for pp for different energies. The red line shows result of fitting, the black one represents experimental data. Left: 100 GeV with data [2], Right: 300 GeV with data [3].

Table 4.1: Results of fitting - obtained parameters for different energies.

Energy \sqrt{s} , GeV	100	300
\bar{m}	2.6336	3.5182
\bar{n}^h	1.7966	2.9169
N	3.044	6.6014
Ω	1.88329	1.7471

4.3.1 Involving Gluon Fission

The multiplicity distribution function can be expressed as a superposition of contributions corresponding to different numbers of split gluons. With each successive gluon undergoing fission, the magnitude of the contribution decreases, i.e., $\Omega_1 \gg \Omega_2$. The probability of obtaining n hadrons is given by:

$$\begin{aligned}
 P_n = & \Omega_1 \sum_{m=1}^{M_{G1}} e^{-\bar{m}} \frac{\bar{m}^m}{m!} C_{mN}^{n-2} \left(\frac{\bar{n}^h}{N} \right)^n \left(1 - \frac{\bar{n}^h}{N} \right)^{mN-n} \\
 & + \Omega_2 \sum_{m=1}^{M_{G2}} e^{-\bar{m}} \frac{\bar{m}^m}{m!} C_{2mN}^n \left(\frac{\bar{n}^h}{N} \right)^n \left(1 - \frac{\bar{n}^h}{N} \right)^{2mN-n}
 \end{aligned} \tag{54}$$

In this expression, the first term represents hadronization resulting from a single gluon, whereas the second term accounts for hadronization following gluon fission.

Figure 7 illustrates the distribution functions of each individual component as well as their combined effect. The contribution from gluon fission becomes particularly significant in the region of high multiplicity.

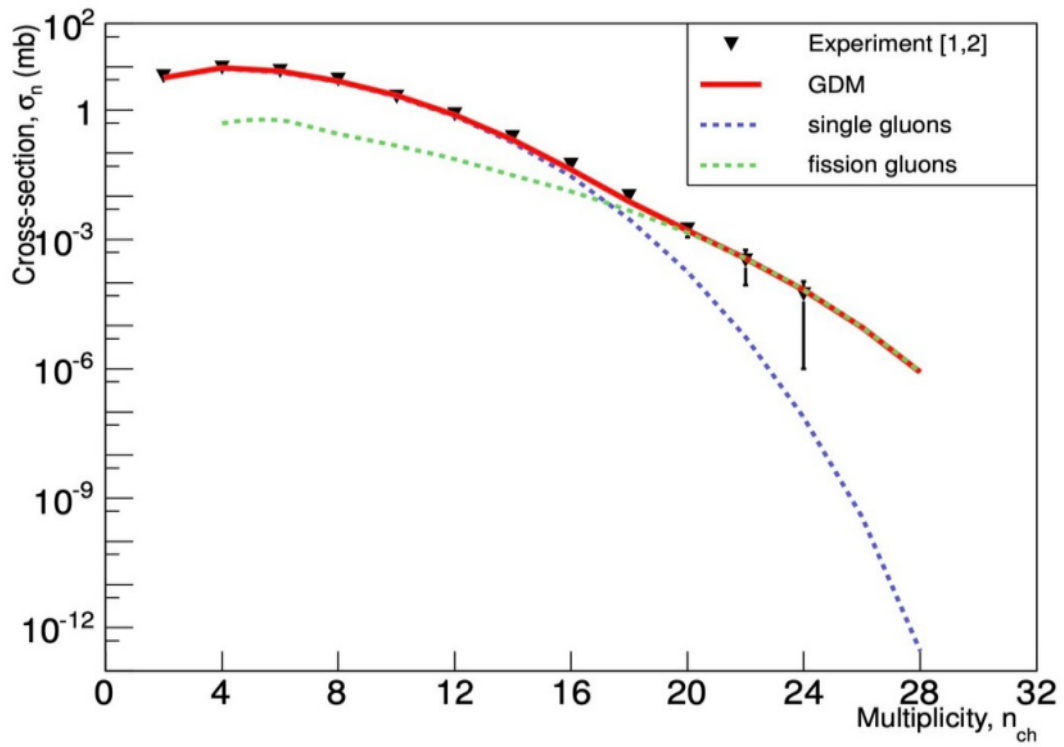


Figure 7: Experimental topological cross sections. The blue line represents contribution of gluons without fission, the green line shows role of gluons with fission. The red line is superposition of both contributions

4.4 Proton-Antiproton Annihilation

The $p\bar{p}$ annihilation process involves a mechanism known as "quark pairing." A proton consists of two up quarks and one down quark (u, u, d), while an antiproton contains the corresponding antiquarks ($\bar{u}, \bar{u}, \bar{d}$). Experimental observations [4] have revealed the formation of three hadronic jets in such annihilation events. The resulting quarks and antiquarks can pair up in various ways to form mesons. For example, the quarks may combine into three neutral mesons ($\bar{u}u, \bar{u}u, \bar{d}d$) or a combination of two charged mesons and one neutral meson ($\bar{u}d, \bar{u}u, \bar{d}u$). Additionally, valence quarks from the initial state may also pair with quark-antiquark pairs that spontaneously emerge from the gluon field.

It is important to note that mesons are generally easier to form than baryons, primarily due to considerations from color confinement in quantum chromodynamics (QCD). All hadrons must be color-neutral, which means the constituent quarks must combine in a way that their color charges cancel out. In this context, it is simpler for a quark to find a single color-matching antiquark to form a meson, rather than finding two additional quarks with the appropriate color combinations to form a baryon. Since mesons consist of two quarks, whereas baryons consist of three, the formation of mesons is statistically more favorable. As a result, most of the hadrons produced in such processes are mesons.

Let us denote the contribution from the process resulting in the production of neutral particles as C_0 , and the contribution from the formation of two charged particles as C_2 . The term C_4 refers to the latter case involving the appearance of sea quarks. The overall multiplicity distribution should account for the contributions from each of these processes.

$$\begin{aligned}
 P_n = & C_0 \sum_{m=1}^{M_G} \frac{e^{-\bar{m}} \bar{m}^m}{m!} C_m^N \left(\frac{\bar{n}^h}{N}\right)^n \left(1 - \frac{\bar{n}^h}{N}\right)^{MN-n} \\
 & + C_2 \sum_{m=1}^{M_G} \frac{e^{-\bar{m}} \bar{m}^m}{m!} C_m^{n-2} \left(\frac{\bar{n}^h}{N}\right)^{n-2} \left(1 - \frac{\bar{n}^h}{N}\right)^{MN-(n-2)} \\
 & + C_4 \sum_{m=1}^{M_G} \frac{e^{-\bar{m}} \bar{m}^m}{m!} C_m^{n-4} \left(\frac{\bar{n}^h}{N}\right)^{n-4} \left(1 - \frac{\bar{n}^h}{N}\right)^{MN-(n-4)}
 \end{aligned} \tag{55}$$

Experimental data [4] yield the contribution ratio $C_0 : C_2 : C_4 = 15 : 40 : 0.05$. The dominant process involves two charged particles, while neutral-only topologies contribute less, and sea quark interactions are largely suppressed.

Conclusion

This dynamics of particle annihilation and hadronization through the framework of the Two Stage Model and the Gluon Dominance Model (GDM). By integrating concepts from QCD and Markov branching processes, we have developed a comprehensive approach to describe both electron-positron annihilation and proton-antiproton interactions. The model successfully accounts for the complex interplay of valence quarks and gluons in pp -collisions, while also providing insights into the hadronization process through various calculation methods, including those with and without gluon fission.

The derivation of generation functions and multiplicity distributions, revealing significant contributions from Binomial, Poisson, and Furry distributions. The analysis of second correlated moments in electron-positron annihilation has provided deeper understanding of the underlying physics. Furthermore, the study has extended to $p\bar{p}$ annihilation, where quark pairing into leading particles (pions) plays a crucial role in determining the final hadronic states.

Advanced topics such as the three-gluon decay of bottomium and the simulation of hadronization parameters using CERN Root Software have been investigated, demonstrating good agreement between theoretical predictions and experimental data. The examination of intermediate charge topologies in pp interactions has further enriched our understanding of these processes.

This work not only consolidates existing knowledge from Giovannini's contributions but also provides a unified framework for analyzing different annihilation scenarios, offering valuable tools for future research in high-energy particle physics.

Bibliography

1. Charged multiplicity distribution and correlations in e^+e^- annihilation at PETRA energies (TASSO Collaboration, 1989) // *Z.Phys.C - Particles and Fields* **45**, 193-208
2. π^+p , K^+p and pp topological cross sections and inclusive interactions at 100 GeV using a hybrid bubble-chamber –spark-chamber system and a tagged beam (W. M. Morse, V. E. Barnes, D. D. Carmony, R. S. Christian, A. F. Garfinkel, and L. K. Rangan; A. R. Erwin, E. H. Harvey, R. J. Loveless, and M. A. Thompson; 1977) // *Physical Review D*; Volume 15, Number 1
3. pp interactions at 300 GeV/c: Measurement of the charged-particle multiplicity and the total and elastic cross section (A. Firestone, V. Davidson, D. Lam, F. Nagy, C. Peck, and A. Sheng; F. T. Dao, R. Hanft, J. Lach, E. Malamud, and F. Nezrick; 1974) // *Physical Review D*; Volume 10, Number 7
4. STUDY OF MULTIPARTICLE PRODUCTION BY GLUONDOMINANCE MODEL (E.S. Kokoulina, V.A. Nikitin) // [arXiv.org/abs/hep-ph/0502224v1](https://arxiv.org/abs/hep-ph/0502224v1) 24 Feb 2005
5. High energy antiparticle-particle reaction differences and annihilations (Rushbrooke J.G. and Webber B.R.) // *Physics Reports*, V.44, No. 1., 1-92.
6. QCD jets as Markov branching processes (A. Giovannini, 1979) // *Nuclear Physics B* 161 429-448
7. [arXiv:hep-ph/0308139](https://arxiv.org/abs/hep-ph/0308139), E. Kokolina, V. Nikitin

Appendix

```
1 /*****
2 * *
3 * Copyright (c) 2005 ROOT Foundation, CERN/PH-SFT *
4 *
5 *
6 *****/
7 #include <iostream>
8 #include "TH1.h"
9 #include "TF1.h"
10 #include "TCanvas.h"
11 #include "TSystem.h"
12 #include "TRandom3.h"
13 #include "TMath.h"
14 #include "TGraphErrors.h"
15 #include "Math/MinimizerOptions.h"
16 Double_t fun(Double_t *x, Double_t *par) {
17
18     Int_t MG = 20;
19     Int_t n, k;
20     Double_t K1, K2, K3, K4;
21     Double_t N1, N2, N3, N4, N5, N6, N;
22     n = x[0];
23     Double_t S, K, C, Sum;
24     Double_t P0, PN, Pn;
25     K1=par[0]+par[1]; // kp+m_
26     K2=par[0]/K1; // kp/(kp+m_)
27     K3=par[1]/K1; // m_/(kp+m_)
28     K4=TMath::Power(K2, par[0]); // (kp/(kp+m_)) ^kp
29     N1=par[2]/par[3]; // nh/N
30     N2=1.-N1; // 1-nh/N
31     N3=N1/N2; // (nh/N)/(1-nh/N)
32     N5=TMath::Power(N2, 2.*par[3]); // (1-nh/N) ^2N
33     S=1.;
34     // m=0
35     for (int i=0; i<n; i++)
```

```

36 {S=S*(2.*par[3]-i)*N3/(i+1.);} // ((nh/N)/(1-nh/N))^n*2N(2N-1)...(2N
    -n+1)/n!
37 P0=par[5]*K4*S*N5;
38
39 Sum=0.;
40 // m=1,2...
41 for (int m=1; m<=MG; m++)
42 {
43     K=1.;
44     for (int l=1; l<=m; l++)
45         {K=K*(par[0]+l-1.)*K3/l;} // (m_/(kp+m_))^m*kp(kp+1)...(kp+m-1)/m!
46     C=1.;
47     for (int p=1; p<=n; p++)
48         {C=C*N3*((2.+par[4]*m)*par[3]-p+1.)/p;} // (2+am)N((2+am)N-1)...((2+
            am)Nn+1)/n!*((nh/N)/(1-nh/N))^n
49
50     N=TMath::Power(N2, (2.+par[4]*m)*par[3]); // (1-nh/N)^(2+am)N
51     Sum=Sum+C*K*N;
52 }
53
54 PN=par[5]*K4*Sum;
55 Pn=PN+P0;
56 return Pn ;
57 }
58 void ee22() {
59     const Int_t npar = 6;
60     TF1 *f1 = new TF1("f1", fun, 2, 28, 6);
61     f1->SetParameter(0, 4.91);
62     f1->SetParameter(1, 3.01);
63     f1->SetParameter(2, 4.34);
64     f1->SetParameter(3, 10.2);
65     f1->SetParameter(4, 0.2);
66     f1->SetParameter(5, 2.0);
67
68     Double_t xvalues1[14] = {2., 4., 6., 8., 10., 12., 14., 16., 18.,
        20., 22., 24., 26.,
69 28.};
70     Double_t yvalues1[14] = {0.1631, 1.7797, 7.8243, 16.7981, 22.9196,
        21.5560, 14.5702,
71 8.2160, 3.6614, 1.6538, 0.5892, 0.1637, 0.0697, 0.0355};
72     Double_t evalues1[14] = {0.0895, 0.2557, 0.5185, 0.7497, 0.8749,
        0.8332, 0.6494,
73 0.4705, 0.2927, 0.1931, 0.1048, 0.0513, 0.0312, 0.0253};
74     for (int k=0; k<14; k++)
75
76     {
77         yvalues1[k] = yvalues1[k]/100.;
78         evalues1[k] = evalues1[k]/100.;
79     }

```

```
80
81 TGraphErrors *gr1 = new TGraphErrors(14, xvalues1, yvalues1, 0,
    evalues1);
82 ROOT::Math::MinimizerOptions::SetDefaultMinimizer("Fumili2");
83 // ROOT::Math::MinimizerOptions::SetDefaultMinimizer("Minuit2");
84 gr1->SetTitle("Multiple Distribution, 22 GeV");
85 gr1->Fit("f1");
86 gr1->Draw("ACP");
87 gr1->SetLineWidth(1);
88 gr1->SetMarkerStyle(20);
89 gr1->SetMarkerSize(1);
90 gr1->SetLineColor(1);
91 f1->SetLineWidth(3);
92 f1->SetLineColor(2);
93 TLegend *leg = new TLegend(0.5,0.8,0.7,0.89);
94 leg->AddEntry(gr1,"Pn");
95 leg->AddEntry(f1,"fitting");
96 leg->Draw();
97 }
```